Journal of Civil Engineering and Construction 2021;10(3):163-176
https://doi.org/10.32732/jcec.2021.10.3.163

Dynamic Impact Factor Determination of an Existing Pre-stressed Concrete I-Girder Bridge Using Vehicle-Bridge Interaction Modelling

Shuvrodeb Adhikary[1], Shohel Rana[2], Jerin Tasnim[1], Nazrul Islam[2]

1. Bangladesh University of Engineering & Technology, Dhaka, Bangladesh
2. Department of Civil Engineering, Bangladesh University of Engineering & Technology, Dhaka, Bangladesh
E-mail: shuvro.bcc1603@gmail.com; shohel@ce.buet.ac.bd; jtria786@gmail.com; nazrulislam@ce.buet.ac.bd

Received: 25 March 2021; Accepted: 27 April 2021; Available online: 5 July 2021

Abstract: The dynamic Impact Factor (IM) of a bridge is influenced by many factors, including Vehicle-Bridge Interaction (VBI), vehicle speed and road roughness. This paper represents the dynamic effects of moving vehicles and the determination of IM of an existing Pre-stressed concrete I-girder bridge utilizing VBI modeling. Evaluation of the IM is expected to provide valuable information for condition assessment and management of the existing bridge. The interaction problem between the vehicle and the bridge includes a dynamic model for the bridge structure subsystem, a dynamic model for the vehicle subsystem, interaction constraints, road roughness modelling and numerical solution techniques for the dynamic systems. The Half-car model is utilized for modelling of the vehicle dynamics and the bridge dynamic model is idealized according to Finite Element Method (FEM). Then FEM along with the mode superposition method are utilized for determining the Equation of Motion (EOM) for the bridge subsystem. D'Alembert's principle is used for developing EOM for the vehicle subsystem. The interaction between vehicle vibration and bridge vibration is established through the contact forces between the wheels and the bridge by employing the compatibility relationship between the contact points and by applying the static equilibrium condition. Lastly, Newmark's-β method is used for solving the coupled mathematical model of the vehicle and bridge interaction problem to determine the responses of the two sub-systems. The whole procedure is then performed for different vehicle speeds and various bridge deck surface roughness conditions to determine the dynamic impact on the existing I-girder bridge named Teesta Bridge located in Bangladesh.
Keywords: Dynamic impact factor; Vehicle bridge interaction; Half-car vehicle model; Bridge dynamic response; Finite element method; Newmark's-β method.

1. Introduction

In the last years, the ever-growing span length of bridges and the increase of vehicle loads and vehicle speeds have led to the consequent increase in dynamic influence on bridge structures [1]. The dynamic effects produced by vehicles passing over the bridge structures and viaducts result in the increase of dynamic forces and displacements over that of the static responses [2]. This phenomenon is known as Dynamic Impact on bridges which is generally considered as Impact Factor (IM) or Dynamic load allowance (DLA) in the bridge design standards. It is calculated as the percent difference between the maximum dynamic responses to the maximum static response. The dynamic impact on bridges depends on various factors such as the dynamic characteristics of bridges, the dynamic characteristics of vehicles, vehicle speeds, the road roughness conditions and, finally the Vehicle-Bridge Interactions (VBI). In earlier research for developing bridge design code, field or experimental test results were used to develop the empirical formulas of IM. However, consideration of all those influencing factors were not possible in the field test. Moreover, due to the limitation of theoretical and computational technologies, those effects were difficult to investigate in the past. Therefore, the dynamic impact due to traffic loads on the existing bridges which were designed with earlier bridge design standards are required to be investigated considering the vibration mechanism between the bridge and vehicles by incorporating all those complex factors.

To assess the dynamic effect of traffic loads, the research on vehicle-bridge interaction phenomena has been performed for decades [3, 4]. Moreover, the research considering the dynamic responses of bridges are performed to assess the fatigue life of the bridges [5], environmental issues [6], safety and comfort of the passengers [7] and also for damage identification of bridges [8]. A lot of research has been performed for the study of vehicle-bridge interaction problems. Ayre et al. [9] and Ayre and Jacobsen [10] first studied the dynamic responses of two-span beam models under moving load. Vellozzi [11] presented the vibration of suspension bridges under the moving load. Frýba [12-13] considered the vehicle and the bridge as a coupled system and derived the analytic solutions when the beam subjected to moving loads. Henchi et al. [14] studied the dynamic response of a bridge-vehicle

interaction system and proposed an algorithm for the dynamic analysis of the coupled system. Yang [15] simplified the effect of the vehicle as two sets of concentrated forces and studied the dynamic responses of the bridge. Chen et al. [16] studied the effect of varying speed when the sprung-mass model is moving on a simply supported beam. Blejwas et al. [17] proposed a solution to solve the interaction problem using Lagrange's equation with multipliers and constraint equation. Various methods of solving the vehicle bridge interaction problems have also been reported (Galdos et al. [18], Yang and Lin [19], Chu et al. [20], Yang and Duan [21]).

Using the vehicle bridge interaction theory, the dynamic impact on bridges has also been studied as presented in the review paper by Deng et al. [22]. Deng and Cai [2, 23] studied dynamic impact factor for evaluating the performance of the bridges. Chen and Wu [24] researched the effect of wind and bridge length on bridge vehicle interaction. Cai et al. [25] studied the influence of approach span condition on slab-on-girder bridges. Li et al. [26] studied the dynamic response of a highway bridge subjected to moving vehicles and observed that the dynamic impact increases with vehicle speed and depends on road roughness conditions. Huang et al. [27] analyzed the impact of vehicles on multi-girder steel bridges with different span lengths. Deng et al. [3] found that the impact on continuous bridges is larger than those of simply supported bridges. Zhu and Law [28] also studied the continuous bridge and vehicle interaction to investigate the dynamic load effects. Mohseni et al. [29] conducted an extensive numerical study to evaluate the influence of some key parameters on the dynamic impact factors for skew composite concrete-steel slab-on-girder bridges and proposed that apart from AASHTO [30] bridge design specification, all the current design specifications for considering IM are un-conservative. Pieraccini et al. [31] performed an experimental study to assess the IM of a railway bridge using the interferometric radar sensor. Gao et al. [32] investigated numerically the dynamic load allowance characteristics of a concrete-filled steel tube (CFST) arch bridge and some conclusions are drawn for evaluating the condition of CFST arch bridges.

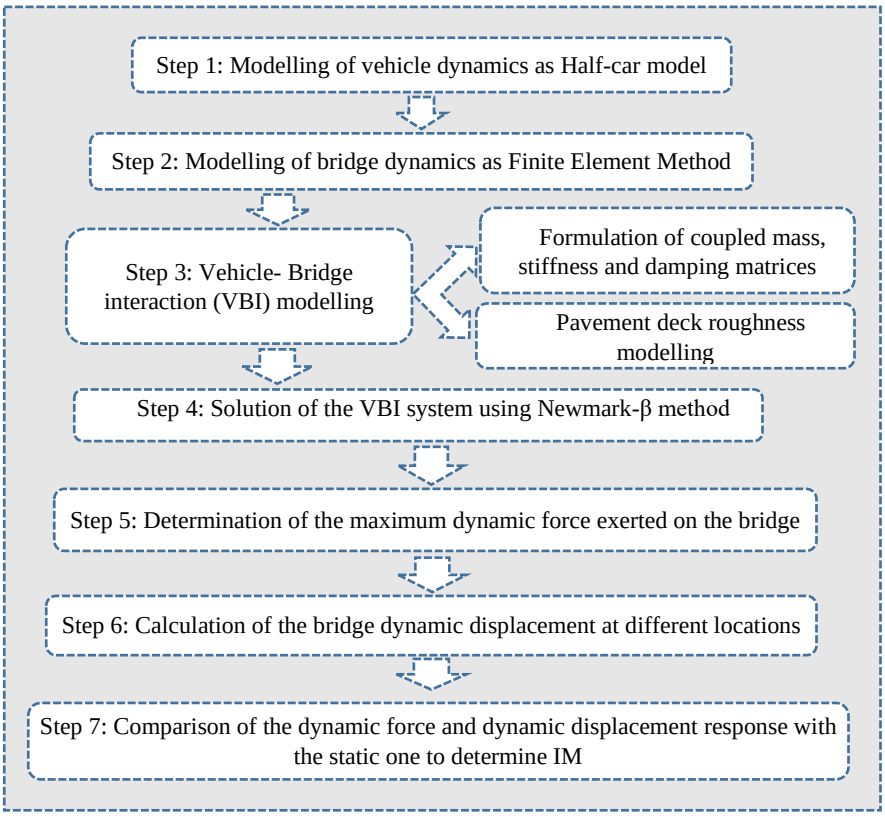

Figure 1. Flow chart of the methodology

As mentioned earlier, estimation of dynamic impact factor is a complicated task because of vehicle-bridge interaction mechanism associated with a large number of influencing parameters, including the dynamic characteristics of both the bridge and the vehicle, road surface condition, vehicle speed etc. Accurate evaluation of the impact factor utilizing the recent theoretical and computational development may lead to valuable information for condition evaluation and management of existing bridges which were designed following the earlier bridge design codes. In this paper, the dynamic behavior of an existing Pre-stressed concrete (PC) I-girder bridge structures under moving vehicle is investigated numerically considering all the complex factors mentioned above and finally the dynamic impact factor is determined. A medium span PC I-girder bridge which is a very common bridge type in Bangladesh is considered as a case study bridge which was designed with earlier bridge

design standard without considering VBI. The bridge is named as Teesta Bridge which is situated in Rangpur district of Bangladesh. The paper is organized by the following main sections. Firstly, the dynamic behavior of vehicle and bridge, modelling and solution of the interaction between the bridge and the vehicle moving over it are presented considering the influence of different vehicle speeds and various extents of pavement roughness. Later, the dynamic impact factor is analyzed following the numerical investigation of the dynamic behavior of the bridge. The methodology of this study is shortly described with a flow chart as in Fig. 1.

2. Vehicle modelling

Modelling of a real vehicle is a very complex task. As a result, in literature, the Half-car model are frequently used for modelling vehicle dynamics as the model is much capable of representing various real vehicle experiences like effect of suspension, energy dissipation, pitching effect [33-36]. For this reason, in this study, a Half-car model is considered as the design vehicle as in Fig. 2. The vehicle model has four Degrees of Freedoms (DOFs). Among them, the body of the vehicle has two DOFs, vertical vehicle body displacement, y_s and pitching rotation, θ_s. The front and rear wheel have also a set of DOFs for vertical displacement, y_{t1} and y_{t2} respectively. Then, a set of kinetic equilibrium functions are formulated for each DOF according to Alembert's principle. The formulation is based on the existing literature [34-36] as shown in Eqns. (1) to (4) respectively.

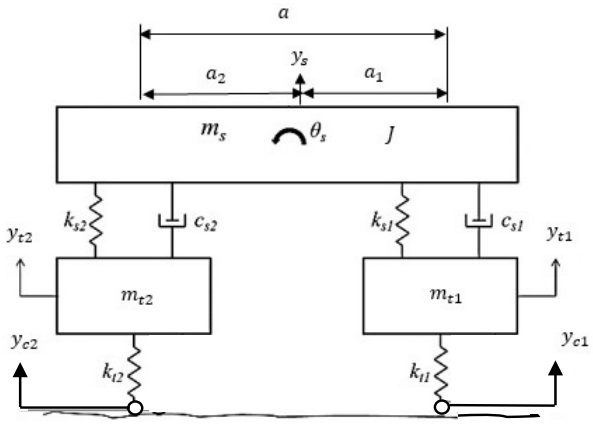

Figure 2. Half-car vehicle model

For vehicle body vibrations up and down:

$$m_s\ddot{y}_s + c_{s1}(\dot{y}_s - \dot{y_{t1}} + \dot{\theta}a_1) + c_{s2}(\dot{y}_s - \dot{y}_{t2} - \dot{\theta}a_2) + k_{s1}(y_s - y_{t1} + \theta a_1) + k_{s1}(y_s - y_{t2} - \theta a_2) = 0 \quad (1)$$

For vehicle body nodes vibration:

$$J\ddot{\theta} + k_{s1}a_1(y_s - y_{t1} + \theta a_1) - k_{s2}a_2(y_s - y_{t2} - \theta a_2) + c_{s1}a_1(\dot{y}_s - \dot{y}_{t1} + \dot{\theta}a_1) - c_{s2}a_2(\dot{y}_s - \dot{y}_{t2} - \dot{\theta}a_2) = 0 \quad (2)$$

For front axle vertical vibration:

$$m_{t1}\ddot{y}_{t1} - k_{s1}(y_s - y_{t1} + \theta a_1) - c_{s1}(\dot{y}_s - \dot{y}_{t1} + \dot{\theta}a_1) + k_{t1}(y_{t1} - y_{c1}) = 0 \quad (3)$$

For rear axle vertical vibration:

$$m_{t2}\ddot{y}_{t2} - k_{s2}(y_s - y_{t1} + \theta a_2) - c_{s2}(\dot{y}_s - \dot{y}_{t2} + \dot{\theta}a_2) + k_{t2}(y_{t2} - y_{c2}) = 0 \quad (4)$$

where, m_s is the mass of the body and the frame of the vehicle; m_{t1} and m_{t2} are the mass of the axle between the front and rear wheel set and tires; k_{s1}, k_{s2}, c_{s1}, c_{s2} are the suspension stiffness and suspension damping between wheel set and the body of the vehicle; k_{t1}, k_{t2}, are the stiffness of the front and rear tires respectively; a_1, a_2 are the distances from the center of gravity to the front wheel and rear wheel. y_{c1}, y_{c2} are the vertical contact point displacements of the wheels on the bridge. Eqns. (1-4) are represented as matrix form as in Eq. (5).

$$[M_v]\{\ddot{y}_v(t)\} + [C_v]\{\dot{y}_v(t)\} + [K_v]\{y_v(t)\} = \{F_v\} \quad (5)$$

where, $[M_v]$is the mass matrix, $[C_v]$ is damping matrix, $[K_v]$ is the stiffness matrix, $\{y_v(t)\}$ is the DOF vector, $\{F_v\}$ is the exciting force of the vehicle vibration. Here,

$$[M_v] = \begin{bmatrix} m_s & 0 & 0 & 0 \\ 0 & J & 0 & 0 \\ 0 & 0 & m_{t1} & 0 \\ 0 & 0 & 0 & m_{t2} \end{bmatrix} \tag{6}$$

$$\{y_v\} = \begin{Bmatrix} y_s \\ \theta \\ y_{t1} \\ y_{t2} \end{Bmatrix} \tag{7}$$

$$[K_v] = \begin{bmatrix} k_{s1} + k_{s2} & k_{s1}a_1 - k_{s2}a_2 & -k_{s1} & -k_{s2} \\ k_{s1}a_1 - k_{s2}a_2 & k_{s1}a_1^2 + k_{s2}a_2^2 & -k_{s1}a_1 & k_{s2}a_2 \\ -k_{s1} & -k_{s1}a_1 & k_{s1} + k_{t1} & 0 \\ -k_{s2} & k_{s2}a_2 & 0 & k_{s2} + k_{t2} \end{bmatrix} \tag{8}$$

$$[C_v] = \begin{bmatrix} c_{s1} + c_{s2} & c_{s1}a_1 - c_{s2}a_2 & -c_{s1} & -c_{s2} \\ c_{s1}a_1 - c_{s2}a_2 & c_{s1}a_1^2 + c_{s2}a_2^2 & -c_{s1}a_1 & c_{s2}a_2 \\ -c_{s1} & -c_{s1}a_1 & c_{s1} & 0 \\ -c_{s2} & c_{s2}a_2 & 0 & c_{s2} \end{bmatrix} \tag{9}$$

3. Modelling of bridge

The Teesta Bridge is located in the northern part of Bangladesh. It is situated in Rangpur District of Bangladesh on Rangpur-Kurigram Highway. The length and width of the bridge are 750 m and 12.11 m respectively. It is a two lane bridge and the bridge system consists of precast girders made composite with cast-in situ 200 mm thick reinforced concrete deck slab [37]. It is consists of 15 nos. of medium span (50 m) simply supported PC I-girder bridges. The bridge is modelled according to FEM as shown in Fig. 3 which consists of constant flexural rigidity, *EI* along the span, where, E is Young's modulus, I is the moment of inertia of the bridge cross section, m is the mass per unit length of span. The equation of motion (EOM) of the bridge is expressed in Eq. (10).

$$[M_b]\{\ddot{y}_b(t)\} + [C_b]\{\dot{y}_b(t)\} + [K_b]\{y_b(t)\} = \{F_b(x,t)\}\delta(x - vt) \tag{10}$$

Where, $[M_b]$is the mass matrix, $[C_b]$ is damping matrix, $[K_b]$ is the stiffness matrix of the bridge, $F_b(x,t)$ is the coupled forces on the bridge and $\{y_b(t)\}$ is the vertical bridge displacement at nodal points at time t and δ is the function of Dirac.

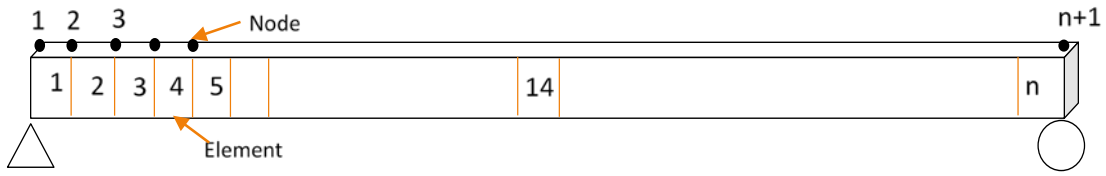

Figure 3. FE model of the bridge

Nevertheless, the dynamic response of a structure is in fact, controlled mainly by some low order modes of vibration. Therefore, generally, a few lowest modes are often enough to obtain a satisfied result when the superposition method is used. Hence, the computational efficiency can be considerably increased. By taking *N* number of vibration modes, the DOF of the bridge will decrease to *N*, and the bridge displacement can be calculated as in Eq. (11) using *N*-order motion equations using method of mode superposition.

$$y_b(x,t) = \{\ddot{y}_b(t)\} = \sum_{i=1}^{N} \{\varphi_i\}\eta_i(t) = [\varphi]\{\eta(t)\} \tag{11}$$

where, $\{\varphi_i\}$ is the vibration mode shape of the bridge and $\eta_i(t)$ is modal co-ordinates. Replacing Eq. (11) into Eq. (10), the EOM of the bridge in modal co-ordinate is obtained as in Eq. (12). Multiplying both side of Eq. (12)

by $\{\varphi_n\}^T$, Eq. (13) is obtained and after applying modal orthogonality principal ($\{\varphi_n\}^T[M]\{\varphi_i\} = 0$, $\{\varphi_n\}^T[M]\{\varphi_n\} = M_n$; $\{\varphi_n\}^T[K]\{\varphi_i\} = 0, \{\varphi_n\}^T[K]\{\varphi_n\} = K_n$) [38], the N uncoupled second order differential equations in modal co-ordinates are obtained as in Eq. (14).

$$[M_b][\varphi]\{\ddot{\eta}(t)\} + [C_b][\varphi]\{\dot{\eta}(t)\} + [K_b][\varphi]\{\eta(t)\} = -\{F_b(x,t)\}\delta(x - vt) \quad (12)$$

$$\{\varphi_n\}^T[M_b][\varphi]\{\ddot{\eta}(t)\} + \{\varphi_n\}^T[C_b][\varphi]\{\dot{\eta}(t)\} + \{\varphi_n\}^T[K_b][\varphi]\{\eta(t)\} = -\{\varphi_n\}^T\{F_b(x,t)\}\delta(x - vt) \quad (13)$$

$$\ddot{\eta}_n(t) + 2\zeta_n\omega_n\dot{\eta}_n(t) + \omega_n^2\eta_n(t) = -\frac{1}{M_n}\{\varphi_n\}^T\{F_b(x,t)\}\delta(x - vt) \;\; n = 1,2,3,\dots\dots\dots\dots\dots, N \quad (14)$$

where, ω_n = natural frequency of vibration mode; M_n, ζ_n = modal mass, and modal damping ratio of n[th] mode respectively; if $x = vt, \delta(x - vt) = 1$ else 0.

The natural frequencies and vibration mode shapes of the bridge are determined by solving the Eigen-value problem of the bridge. Static condensation is applied for having reduced mass and stiffness matrix related to only translational DOF. The stiffness and mass matrices of the bridge are partitioned as in Eq. (15). Then, the reduced matrices are calculated as in Eq. (16). Where, $\hat{\boldsymbol{k}}_{\boldsymbol{tt}}$ = reduced stiffness matrix and $\hat{\boldsymbol{m}}_{\boldsymbol{tt}}$ = reduced mass matrix corresponding only to the translational DOFs. The Eigen-value problem is formulated in Eq. (17) and the Eigen parameters (i.e., natural frequencies and mode shapes) of the bridge are calculated by using Eigen solution.

$$[K_b] = \begin{bmatrix} k_{tt} & k_{ot} \\ k_{to} & k_{oo} \end{bmatrix}, [M_b] = \begin{bmatrix} m_{tt} & m_{ot} \\ m_{to} & m_{oo} \end{bmatrix} \quad (15)$$

$$\hat{k}_{tt} = k_{tt} - k_{ot}^T k_{oo}^{-1} k_{ot}, \hat{m}_{tt} = m_{tt} \quad (16)$$

$$\left[[\hat{k}_{tt}] - \omega_r^2[\hat{m}_{tt}]\right]\{\phi_r\} = \{0\} \quad (17)$$

4. Vehicle bridge interaction

Now, two sets of differential equations have been developed as in Eq. (5) and (14). One of which is for the vehicle as in Eq. (5) and another set is for the bridge as in Eq. (14). For developing interaction between the vehicle and the bridge sub-systems, the compatibility conditions are applied at the contact points and the coupled equation of motions are formulated. The effect of pavement roughness is incorporated here as wheel displacement are the resultant of both pavement roughness and bridge displacement as in Eqns. (18-19) where the wheel vertical displacement, y_{c1} and y_{c2} are calculated. The forces on the bridge consist of the weight of vehicle and wheel body and the elastic forces as calculated in Eqns. (20-21). These forces result in the coupling between the bridge and vehicle vibration. The coupled vehicle bridge model is shown in Fig. 4.

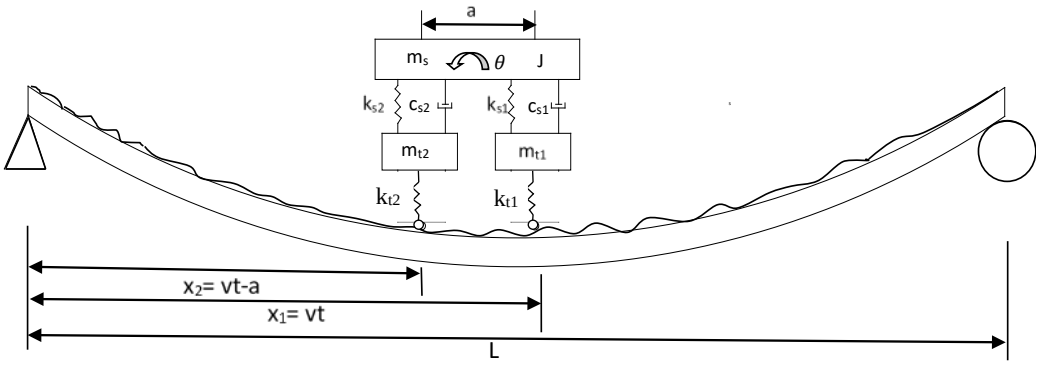

Figure 4. The model of coupled vehicle bridge vibration

$$y_{c1} = y_b(x_1,t) + r(x_1) = \sum_{i=1}^{N}\varphi_i(x_1)\eta_i(t) + r_1 \quad (18)$$

$$y_{c2} = y_b(x_2,t) + r(x_2) = \sum_{i=1}^{N}\varphi_i(x_2)\eta_i(t) + r_2 \qquad (x_2 = x_1 - a) \quad (19)$$

$$F_1(x_1,t) = W_1 - K_{t1}(y_{t1} - y_{c1}) \quad (20)$$

$$F_2(x_2,t) = W_2 - K_{t2}(y_{t2} - y_{c2}) \quad (21)$$

where, y_{c1} and y_{c2} are the displacements of the front and rear wheels respectively; r_1 and r_2 are the roughness at the front and rear wheel contact points respectively. $F_1(x_1,t)$ and $F_2(x_2,t)$ are the point forces at the wheel contact points; W is the static load which comprises of sprung weight and un-sprung weight.

Now according to compatibility conditions, the coupling is done within matrix format using equations (1), (2), (3), (4) and (12). Replacing $F_i(x,t)$ from Eqns. (20-21) in Eq. (14), Eq. (26) is obtained. Eqns. (22-26) are converted to a matrix representation as in Eq. (27) which is the coupled matrix formulation of both the vehicle and the bridge subsystems interacting together.

$$m_s\ddot{y}_s + c_{s1}\left(\dot{y}_s - \dot{y_{t1}} + \dot{\theta}a_1\right) + c_{s2}\left(\dot{y}_s - \dot{y}_{t2} - \dot{\theta}a_2\right) + k_{s1}(y_s - y_{t1} + \theta a_1) + k_{s1}(y_s - y_{t2} - \theta a_2) = 0 \tag{22}$$

$$J\ddot{\theta} + k_{s1}a_1(y_s - y_{t1} + \theta a_1) - k_{s2}a_2(y_s - y_{t2} - \theta a_2) + c_{s1}a_1\left(\dot{y}_s - \dot{y}_{t1} + \dot{\theta}a_1\right) - c_{s2}a_2\left(\dot{y}_s - \dot{y}_{t2} - \dot{\theta}a_2\right) = 0 \tag{23}$$

$$m_{t1}\ddot{y}_{t1} - k_{s1}(y_s - y_{t1} + \theta a_1) - c_{s1}\left(\dot{y}_s - \dot{y}_{t1} + \dot{\theta}a_1\right) + k_{t1}(y_{t1} - y_{c1}\delta_1) = 0 \tag{24}$$

$$m_{t2}\ddot{y}_{t2} - k_{s2}(y_s - y_{t1} + \theta a_2) - c_{s2}\left(\dot{y}_s - \dot{y}_{t2} + \dot{\theta}a_2\right) + k_{t2}(y_{t2} - y_{c2}\delta_2) = 0 \tag{25}$$

$$\frac{a_2\varphi_{1n}\delta_1 + a_1\varphi_{2n}\delta_2}{a}m_s\ddot{y}_s + \frac{\varphi_{1n}\delta_1 - \varphi_{2n}\delta_2}{a}J\ddot{\theta} + \varphi_{1n}\delta_1 m_{t1}\ddot{y}_{t1} + \varphi_{2n}\delta_2 m_{t2}\ddot{y}_{t2} + \ddot{\eta}_n + 2\zeta_n\omega_n\dot{\eta}_n + \omega_n^2\eta_n = -(\varphi_{1n}W_1\delta_1 + \varphi_{2n}W_2\delta_2) \tag{26}$$

$$[M(t)]\{\ddot{Y}\} + [C(t)]\{\dot{Y}\} + [K(t)]\{Y\} = \{Q(t)\} \tag{27}$$

Here, $[M(t)]$, $[C(t)]$ and $[K(t)]$ are (n+4) orders coupled time dependent mass, damping and stiffness matrices; $\{Q(t)\}$ is (n+4) order force vector as shown in Eq. (28) and $\{Y\}$ is (n+4) order displacement vector consisting of modal response of bridge combined with vehicle response as shown in Eq. (29). By solving Eq. (27), vehicle responses can be obtained directly from the solution and bridge responses are calculated using Eq. (11).

$$\{Q(t)\} = \begin{Bmatrix} 0 \\ 0 \\ k_{t1}r_1\delta_1 \\ k_{t2}r_2\delta_2 \\ -(\varphi_{11}W_1\delta_1 + \varphi_{21}W_2\delta_2) \\ -(\varphi_{12}W_1\delta_1 + \varphi_{22}W_2\delta_2) \\ \vdots \\ -(\varphi_{1n}W_1\delta_1 + \varphi_{2n}W_2\delta_2) \end{Bmatrix} \tag{28}$$

$$\{Y(t)\} = \begin{Bmatrix} y_s(t) \\ \theta \\ y_{t1}(t) \\ y_{t2}(t) \\ \eta_1(t) \\ \eta_2(t) \\ \vdots \\ \eta_n(t) \end{Bmatrix} \tag{29}$$

5. Bridge deck surface roughness modelling

The wheels of the vehicle are presumed to remain in contact with the bridge deck. Therefore, the displacement of the wheels remain equal to that of the bridge deck at the contact points. The deck surface roughness plays a vital role in stimulating vehicle vibrations which is simulated theoretically. Artificial surface roughness of Class A-B profile according to ISO 8608 classification [39-40] is generated using Eq. (30).

$$r(x) = \sum_{i=0}^{N}\sqrt{\Delta n}.2^k.10^{-3}.\left(\frac{n_0}{i.\Delta n}\right).cos(2\pi.i.\Delta n.x + \varphi_i) \tag{30}$$

Where, L is the length of the road profile and B is the sampling interval; x is the abscissa variable from 0 to L; $\Delta n = 1/L$; $n_{max} = 1/B$; $N = n_{max}/\Delta n = L/B$; k is a constant value which depends on ISO road roughness classification and varies from 3 to 9, corresponding to the road roughness profiles from class A to class H. Also, $n_0 = 0.1$ cycles/m; φ_i is the random phase angle following a uniform probabilistic distribution within 0 to 2π.

6. Determination of dynamic impact factor of the bridge

The equations representing the VBI system are the differential equation set with time-varying coefficients. Numerical analysis is performed here to solve the coupled system. Newmark's β method is used for solving numerically the coupled formulation as in Eq. (27) resulting from the differential equations of bridge and vehicle subsystems. This numerical method breaks the time into different number of steps with an increment of Δt. Δt represents the time required for the vehicle to traverse one bridge element (ΔL) with a vehicle speed (v), where, $\Delta t = \Delta L/v$. In this section, the vehicle induced bridge dynamic responses are analyzed and the dynamic impact factor of the existing I-girder bridge (Teesta Bridge) is determined. The influence of vehicle speed and bridge deck surface roughness are also investigated. The vehicle wheel and the vehicle body will be studied in terms of acceleration and displacement.

6.1 Vehicle and bridge dynamic parameters

The dynamic parameters of the Half-car vehicle model are provided in Table 1 following the references [8, 41]. The vehicle model is based on the H20-44 truck design loadings included in the American Association of State Highway and Transportation Officials (AASHTO) specifications [42].

Table 1. Vehicle dynamic parameters

Element	Notation	Value
Stiffnesses (N/m)		
Front wheel	k_{t1}	1570000
Rear wheel	k_{t2}	3140000
Front suspension	k_{s1}	232000
Rear suspension	k_{s2}	746000
Damping (N-s/m)		
Front suspension	c_{s1}	50000
Rear suspension	c_{s2}	70000
Masses (kg)		
Front axle	m_{t1}	600
Rear axle	m_{t2}	1000
Body	m_s	17000
Rotary Inertia (kg-m^2)	J	90000
Vehicle speed (km/h)	V	40, 60, 80, 100
Distances from C.G.(m)		
From front wheel	a_1	3.8
From rear wheel	a_2	1.5

Teesta Bridge is a simply supported PC I-girder bridge and consists of five girders with 200 mm thick deck slab. Each span of the bridge is 50 m. A single lane of the bridge subjected to one vehicle is considered for the finite element modelling. The flexural rigidity (EI) and mass of the bridge girder is calculated as 6.96×10^{10} Nm^2 and 6818.5 kg/m respectively. 5% modal damping is assumed for the bridge for all the modes. It is to be mentioned that the allowable maximum vehicle speed is 60 km/hr for this bridge.

6.2 Dynamic impact on bridge for front wheel

Using the parameters of vehicle and bridge, the coupled vehicle-bridge interaction problem as in Eq. (27) is solved and the contact point forces are calculated using Eqns. (20-21). Four vehicle speeds are considered such as 40 km/hr, 60 km/hr, 80 km/hr and 100 km/hr.

In this section, a detail description of IM for the first contact point is provided. This study also describes the amplification of the contact point forces on the bridge due to VBI with respect to static vehicle loading. The front wheel contact point force of the vehicle passing the bridge at different speeds are typically shown in Fig. 5. It gives the insight of actual point force on the bridge in a vehicle bridge interaction system. The static point force of front wheel at the first contact point on the bridge is $(\frac{m_s}{a} \times a_2 + m_{t1}) \times g$ or 5.30×10^4 N. Fig. 5 shows that the dynamic contact point force varies on the bridge profile due to VBI which is significantly higher than static contact point

force. The difference between the static point force and the maximum dynamic point force is calculated in Table 2 which varies from 22.5% to 47.2% for different vehicle speeds. It also shows that maximum dynamic force increases rapidly with the increase of vehicle speed.

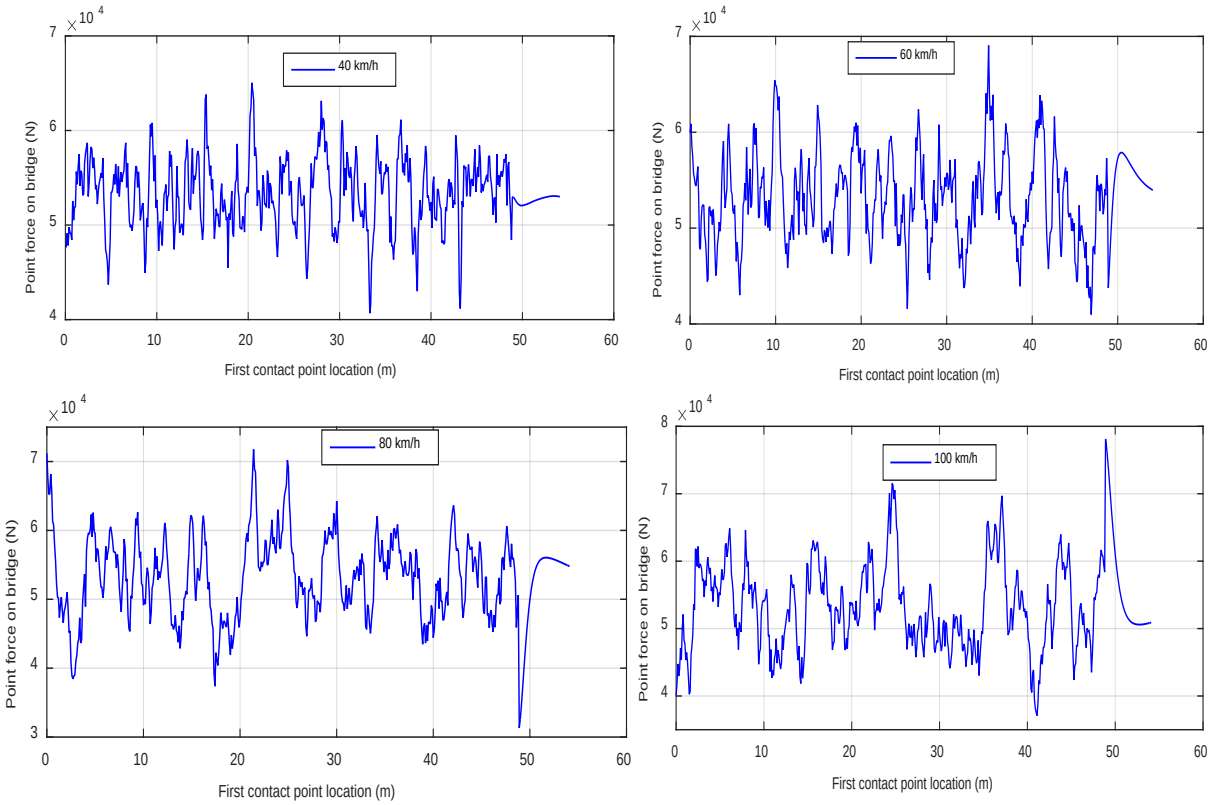

Figure 5. Front wheel contact point forces at different vehicle speeds along the bridge span

Table 2. Front wheel contact point forces

Vehicle speed (kmh-1)	Static Point Force (N)	Maximum Dynamic Point Force (N)	Percent Increase (%)
40	5.30×10^4	6.51×10^4	22.5
60	5.30×10^4	6.91×10^4	30.1
80	5.30×10^4	7.18×10^4	35.2
100	5.30×10^4	7.81×10^4	47.2

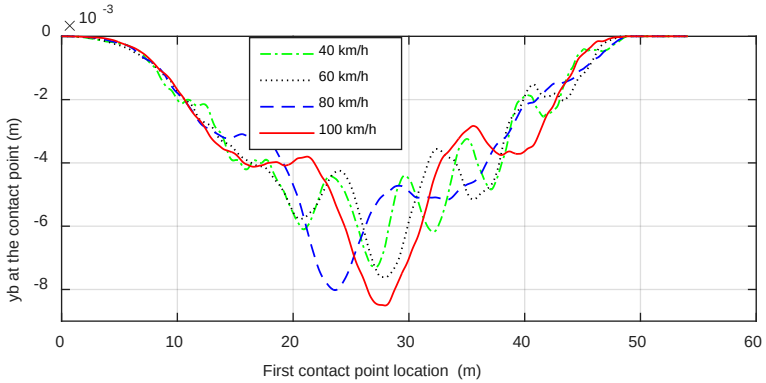

Figure 6. Bridge dynamic displacement at front wheel contact point considering VBI

Now, the vehicle induced dynamic displacement of the bridge is calculated for different vehicular velocities. Fig. 6 displays the vertical displacement (y_b) of bridge at different contact point of the wheel on the bridge considering vehicle bridge interaction obtained from Eq. (27). It also shows the vertical displacement responses of the bridge with the change of vehicle speeds. At lower vehicle speed, due to comparatively lower dynamic

influence, the bridge vertical displacement is less while with the increase of speed, the displacement increases. A finite element software package, SAP2000 [43] is used to obtain the bridge static displacement response at wheel contact points using the built-in moving load analysis program of the software to compare with the dynamic displacement as calculated following the VBI formulation considered in this study. Fig. 7(a) shows the moving static wheel loads on the bridge and Fig. 7(b) represents the maximum vertical displacement envelope of the bridge due to moving static vehicle loads. From Fig. 7(b), the maximum static displacement is calculated which is tabulated in Table 3.

At this point, the dynamic displacement considering VBI and maximum static displacement of the bridge for the given vehicle are available, the dynamic impact factor (IM) for front wheel contact point of the Teesta Bridge is calculated in Table 3. The bridge was built according to AASHTO 2005 [44] bridge standard, where dynamic impact factor was calculated as per Eq. (31), where, L is the length of the bridge in feet, which result in the IM value of 0.176 or 17.6%. However, from Table 3, it is evident that the considerations of bridge deck roughness and also the VBI have result in higher IM than the design IM value used in the bridge.

$$IM = \frac{50}{L+125} \tag{31}$$

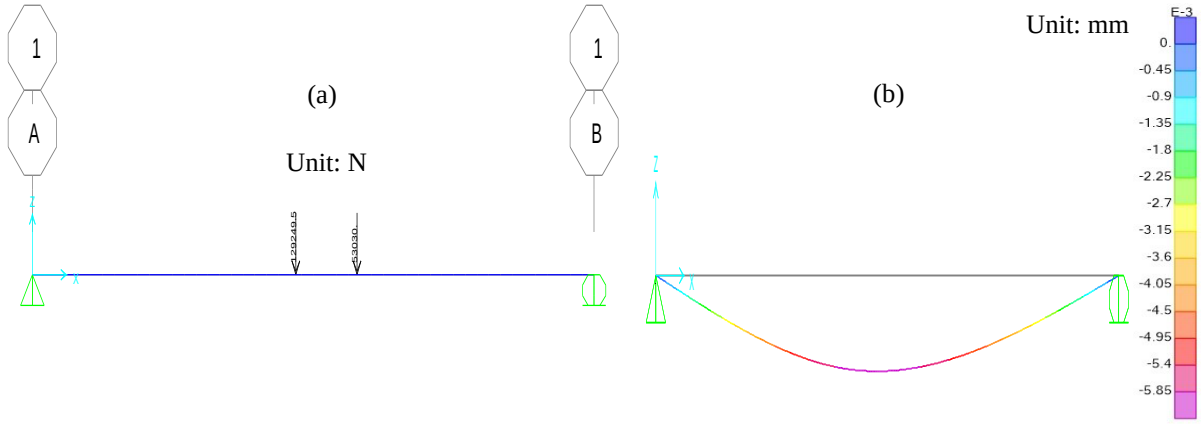

Figure 7. Bridge static displacement due to moving vehicle load

Table 3. Dynamic impact factor (IM) for front wheel contact point

Vehicle speed (kmh-1)	Static Displacement (mm)	Maximum Dynamic Displacement (mm)	IM (%)
40	6.1	7.3	19.7
60	6.1	7.7	26.2
80	6.1	8.0	31.2
100	6.1	8.5	39.3

6.3 Dynamic impact with and without considering VBI

Usually, most of the common finite element software do not consider Vehicle-Bridge Interaction while calculating the dynamic vertical displacement of bridge subjected to moving vehicle load calculated using dynamic time history analysis procedure. In this section, the dynamic impact is compared with and without considering VBI. To determine the dynamic impact without considering VBI, the bridge is modeled using SAP2000 FE software as in Fig. 7(a) and the dynamic time history analysis is performed under moving vehicle load. Fig. 8 displays the comparison between the dynamic displacement response of the bridge with and without considering the VBI for a particular vehicle speed of 80 Kmh^{-1}, where vertical displacement of the bridge is plotted against the first wheel contact point location of vehicle on the bridge. It is evident from Fig. 8 that, there is significant rise in bridge displacement if VBI is considered. Table 4 shows the difference in IM between the two cases.

Table 4. Bridge dynamic deflection with and without consideration of VBI

Type of Analysis	Maximum Dynamic Displacement (mm)	IM (%)
Without VBI	6.5	6.6
With VBI	8.1	32.8

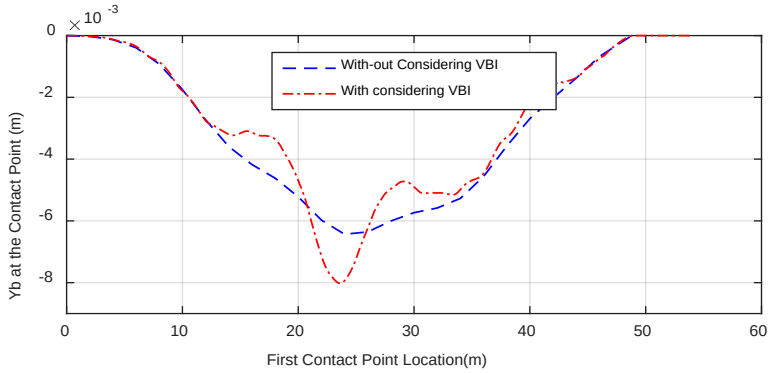

Figure 8. Vertical dynamic displacement of bridge with and without considering VBI

6.4 Dynamic impact on bridge for rear wheel

Similar to the front wheel, the contact point force for the rear wheel also varies throughout the bridge length due to VBI. The static point force for rear wheel at the second contact point on the bridge is $(\frac{m_s}{a} \times a_1 + m_{t2}) \times g$ or 1.29×10^5 N. Fig. 9 shows that the contact point force on the bridge for different vehicle speeds while the rear wheel passes the bridge is neither constant nor equal to the static force. The maximum dynamic force is determined and percent increase as compared to the static force is calculated in the Table 5.

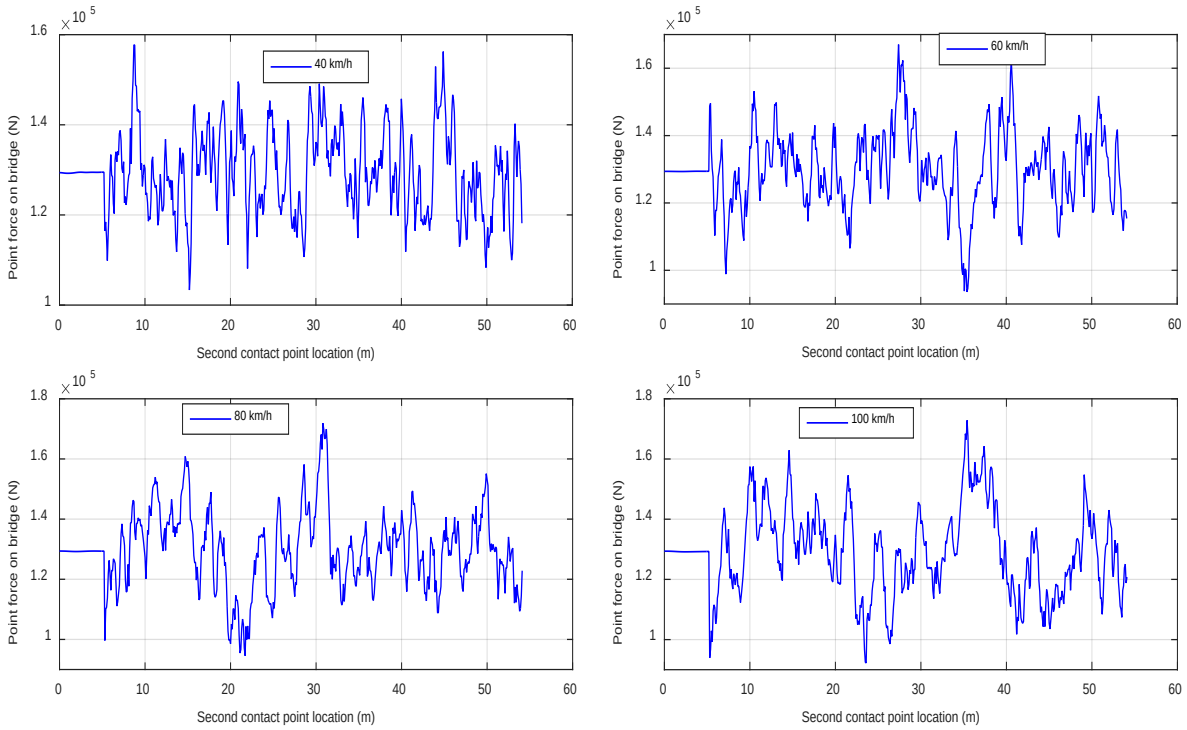

Figure 9. Contact point force of rear wheel along the bridge span

Table 5. Rear wheel contact point forces

Vehicle Speed (kmh-1)	Static Point Force (N)	Maximum Dynamic Point Force (N)	Percent Increase (%)
40	1.29×10^5	1.58×10^5	21.8
60	1.29×10^5	1.67×10^5	29.1
80	1.29×10^5	1.71×10^5	32.2
100	1.29×10^5	1.73×10^5	33.7

The dynamic displacement of the bridge at rear wheel contact point is shown in Fig. 10 for the different vehicle speeds considered in this study. The displacement is much more than the front wheel contact point as higher value of dynamic force is observed on the rear wheel contact point. The displacement curve is not smooth as well due to

variation of dynamic forces over the bridge. Dynamic impact with respect to the static displacement of bridge, is also determined for this case in Table 6. It is understood that dynamic impact of the rear wheel contact point follows the same trend as front wheel contact location with the higher magnitude than previous one as the static force on rear wheel contact point is higher than that of the front wheel.

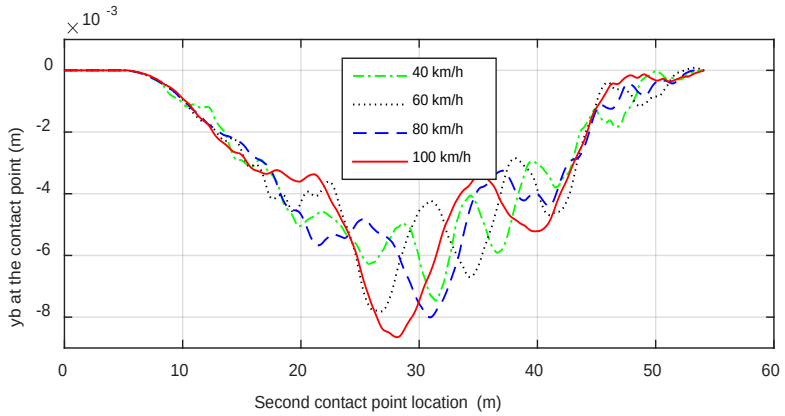

Figure 10. Bridge dynamic displacement at rear wheel contact point

Table 6. Dynamic impact (IM) for rear wheel contact point

Vehicle Velocity (kmh-1)	Static Displacement (mm)	Maximum Dynamic Displacement (mm)	IM (%)
40	6.1	7.4	21.3
60	6.1	7.8	27.9
80	6.1	8.1	32.8
100	6.1	8.7	42.6

6.5 Dynamic impact for different pavement deck surface roughness

For calculation of the dynamic magnification of a bridge, deck surface roughness plays a vital role. Surface characterstics of the deck pavement has influence on the VBI system by increasing the force on the bridge and thereby influencing the dynamic displacement of the bridge. Higher pavement surface roughness will eventually result in increasing the contact force on the bridge which will result in large vertical displacement of the bridge. Four surface roughness conditions are considered as Class A-B, Class B-C, Class C-D and Class D-E. Next, all the calculations are performed similarly as described in the previous sections and finally the dynamic contact point forces and vertical dynamic displacements of the bridge for each roughness cases are determined. Table 7 shows the percent increase in wheel contact forces over static one for various deck surface roughness conditions for a typical vehicle speed of 80 km/h. Fig. 11 shows the bridge contact point dynamic displacement for different roughness conditions. It is observed that the bridge vertical dynamic displacement is comparatively higher for the higher surface roughness condition. The dynamic impact for different roughness conditions are also calculated in Table 8.

Table 7. Dynamic contact point force for different surface roughness

Surface Roughness	Maximum Dynamic Point Force (N)	Percent Increase (%)
Class A-B	7.18×10^4	35.2
Class B-C	8.60×10^4	62.0
Class C-D	1.11×10^5	109.1
Class D-E	1.76×10^5	231.5

Table 8. Dynamic impact for different bridge deck surface roughness

Surface Roughness	Maximum Dynamic Displacement (m)	IM (%)
Class A-B	0.0080	31.2
Class B-C	0.0088	44.3
Class C-D	0.0102	67.2
Class D-E	0.0129	111.8

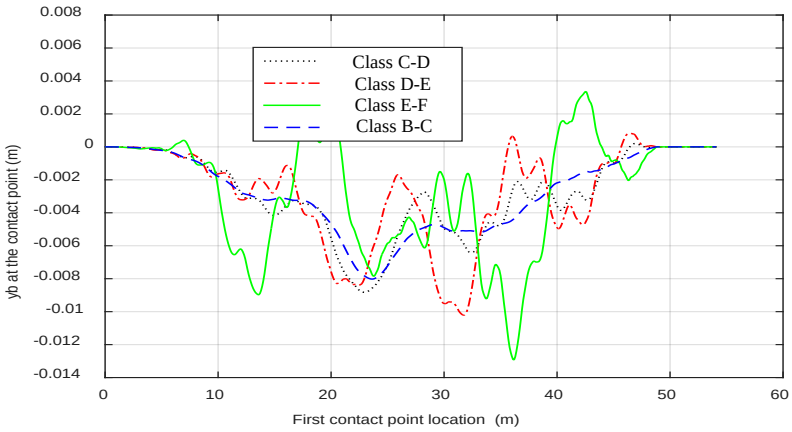

Figure 11. Bridge dynamic displacement under wheel contact point for different surface roughness

7. Conclusions

Pre-stressed Concrete (PC) I-girder bridges are widely used for highways; the dynamic impact factors (IM) of these bridges vary within a wide range. This paper examines the dynamic impact factor of a 50 m span existing PC I-girder Bridge named as Teesta Bridge situated in Bangladesh considering the effect of vehicle bridge interaction phenomenon. The influences of the vehicle travelling speed and bridge deck surface roughness on the impact factor are also investigated. For vehicle bridge interaction modelling, the Half-car vehicle dynamic model is utilized and for the bridge, a discretized finite element model is developed. The coupling between the two subsystems is performed based on compatibility condition at the contact point of the wheel and the bridge which results in a time dependent complex mathematical formulation of the combined system. Newmark-β method, is utilized to solve the coupled formulation to obtain the bridge and the vehicle responses. The conclusions of this study can be drawn as follows:

a) The contact point forces of wheels on the bridge increase significantly due to dynamic effect than that of static wheel loads.

b) The dynamic displacement and IM of the bridge increase with the increase of vehicle speed.

c) The bridge was designed for an impact factor of 17.6%. However, in this study, it is observed that with due consideration of vehicle bridge interaction and pavement surface roughness, the dynamic impact exceeds the designed value for all the vehicle speeds considered.

d) For the allowable speed limit of 60 km/hr for the bridge, the IM is found in the range of 26% to 28% for front and rear wheel contact points. For higher value of vehicle speed, the impact factor keeps rising and for a speed of 100 kmh^{-1}, it becomes more than 40%.

e) The IM for the rear wheel contact is higher than that of front wheel, which infers that with increment in loading the IM also increases.

f) Deck surface roughness also affects the dynamic behavior of the bridge significantly. The impact factor increases with the increase of roughness. Therefore, the deck surface roughness should be kept in good condition to avoid the increase in IM value.

A future work is required to be performed on the implementation of this method in the field experiment to investigate the impact factor of the bridge experimentally.

8. Reference

[1] Xia H, De Roeck G, Goicolea JM. Bridge vibration and controls: new research. Nova Science Publisher, Inc., New York. 2012.

[2] Deng L, Cai CS. Development of dynamic impact factor for performance evaluation of existing multi-girder concrete bridges. Engineering Structures. 2010; 32(1):21-31.

[3] Deng L, He W, Shao Y. Dynamic impact factors for shear and bending moment of simply supported and continuous concrete girder bridges. Journal of Bridge Engineering. 2015; 20(11):04015005.

[4] Huang D. Dynamic analysis of steel curved box girder bridges. Journal of Bridge Engineering. 2001; 6(6):506-513.

[5] Battista RC, Pfeil MS, Carvalho EML. Vehicle-structure interaction effect on the fatigue life of steel orthotropic decks. Proceedings of the 8th International Conference on Structural Dynamics, EURODYN 2011, Leuven, Belgium. 2011 July 4-6. p.1-7.

[6] Akiyama H, Fukada S, Kajikawa Y. Numerical study on the vibrational serviceability of flexible single span bridges with different structural systems under traffic load. Structural Engineering International. 2007; 17(3):256-263.
[7] Chen SR, Cai CS, Levitan M. Understand and improve dynamic performance of transportation system—a case study of Luling Bridge. Engineering structures. 2007; 29(6):1043-1051.
[8] Law SS, Li J. Updating the reliability of a concrete bridge structure based on condition assessment with uncertainties. Engineering Structures. 2010; 32(1):286-296.
[9] Ayre RS, Ford G, Jacobsen LS. Transverse vibration of a two-span beam under action of a moving constant force. J. Appl. Mech. 1950; 17(1):1-12.
[10] Ayre RS, Jacobsen LS. Transverse vibration of a two-span beam under the action of a moving alternating force. J.Appl.Mech. 1950; 17(3):283-290.
[11] Vellozzi J. Vibration of suspension bridges under moving loads. J. Struct. Eng., ASCE. 1967; 93(4):123-138.
[12] Frýba L. Dynamics of railway bridges, 2nd ed. Thomas Telford Publishing, London. 1996.
[13] Fryba, L. Vibrations of solids and structure under moving loads, 3rd ed. Thomas Telford, London.1999.
[14] Henchi K, Fafard M, Talbot M, Dhatt G. An efficient algorithm for dynamic analysis of bridges under moving vehicles using a coupled modal and physical components approach. Journal of Sound and Vibration. 1998; 212(4):663-683.
[15] Yang YB, Yau JD. Vehicle-bridge interaction element for dynamic analysis. Journal of Structural Engineering. 1997; 123(11):1512-1518.
[16] Chen Y, Tan CA, Bergman LA. Effects of boundary flexibility on the vibration of a continuum with a moving oscillator. J. Vib. Acoust. 2002; 124(4):552-560.
[17] Blejwas TE, Feng CC, Ayre RS. Dynamic interaction of moving vehicles and structures. Journal of Sound and Vibration. 1979; 67(4):513-521.
[18] Galdos NH, Schelling DR, Sahin MA. Methodology for impact factor of horizontally curved box bridges. Journal of Structural Engineering. 1993; 119(6):1917-1934.
[19] Yang YB, Lin BH. Vehicle-bridge interaction analysis by dynamic condensation method. Journal of Structural Engineering. 1995; 121(11):1636-1643.
[20] Chu KH, Garg VK, Wang TL. Impact in railway prestressed concrete bridges. Journal of Structural Engineering. 1986; 112(5):1036-1051.
[21] Yang J, Duan R. Modelling and simulation of a bridge interacting with a moving vehicle system. [M.Sc. Eng. Thesis]. Blekinge Institute of Technology, Sweden, 2013.
[22] Deng L, Yu Y, Zou Q, Cai CS. State-of-the-art review of dynamic impact factors of highway bridges. Journal of Bridge Engineering. 2015; 20(5):04014080.
[23] Deng L, Cai CS. Identification of parameters of vehicles moving on bridges. Engineering Structures. 2009; 31(10):2474-2485.
[24] Chen SR, Wu J. Dynamic performance simulation of long-span bridge under combined loads of stochastic traffic and wind. Journal of Bridge Engineering. 2010; 15(3):219-230.
[25] Cai CS, Shi XM, Araujo M, Chen SR. Effect of approach span condition on vehicle-induced dynamic response of slab-on-girder road bridges. Engineering Structures. 2007; 29(12):3210-3226.
[26] Li H, Wekezer J, Kwasniewski L. Dynamic response of a highway bridge subjected to moving vehicles. Journal of Bridge Engineering. 2008; 13(5):439-448.
[27] Huang D, Wang TL, Shahawy M. Impact analysis of continuous multigirder bridges due to moving vehicles. Journal of Structural Engineering. 1992; 118(12):3427-3443.
[28] Zhu XQ, Law SS. Dynamic load on continuous multi-lane bridge deck from moving vehicles. Journal of Sound and Vibration. 2002; 251(4):697-716.
[29] Mohseni I, Ashin A, Choi W, Kang J. Development of dynamic impact factor expressions for skewed composite concrete-steel slab-on-girder bridges. Advances in Materials Science and Engineering. 2018; ID: 4313671.
[30] AASHTO. AASHTO LRFD bridge design specifications: Customary US units. American Association of State Highway and Transportation Officials, Washington, DC, USA, 7th edition. 2014.
[31] Pieraccini M, Miccinesi L, Nejad AA, Fard ANN. Experimental dynamic impact factor assessment of railway bridges through a radar interferometer. Remote Sensing. 2019; 11(19):2207.
[32] Gao Q, Ma Q, Cui K, Li J, Xu C. Numerical investigation of the characteristics of the dynamic load allowance in a concrete-filled steel tube arch bridge subjected to moving vehicles. Shock and Vibration. 2020, Article ID 8819137.
[33] Yang YB, Yau JD, Yao Z, Wu YS. Vehicle-bridge interaction dynamics: with applications to high-speed railways. World Scientific Publishing Co. Pte. Ltd, Singapore. 2004.
[34] Yang YB, Lin CW, Yau JD. Extracting bridge frequencies from the dynamic response of a passing vehicle. Journal of Sound and Vibration. 2004; 272(3-5):471-493.

[35] Yang YB, Yau JD. Vehicle-bridge interaction element for dynamic analysis. Journal of Structural Engineering. 1997; 123(11):1512-1518.
[36] Feng D, Sun H, Feng MQ. Simultaneous identification of bridge structural parameters and vehicle loads. Computers & Structures. 2015; 157:76-88.
[37] Bureau of Research Testing & Consultation (BRTC). Teesta bridge project report. File No. 1247, Dept. of Civil Engineering Library, Bangladesh Univ. of Engineering and Technology, Dhaka, Bangladesh. 2007.
[38] Chopra, AK. Dynamics of structures, 4th ed. Prentice Hall, New Jersey. 2012.
[39] Múčka P. Simulated road profiles according to ISO 8608 in vibration analysis. Journal of Testing and Evaluation. 2017; 46(1):405-418.
[40] Agostinacchio M, Ciampa D, Olita S. The vibrations induced by surface irregularities in road pavements–a Matlab® approach. European Transport Research Review. 2014; 6(3):267-275.
[41] OBrien EJ, Cantero D, Enright B, González A. Characteristic dynamic increment for extreme traffic loading events on short and medium span highway bridges. Engineering Structures. 2010; 32(12):3827-3835.
[42] AASHTO. AASHTO-LRFD Bridge design specifications. American Association of State Highway and Transportation Officials, Washington DC, 6th edition. 2012.
[43] SAP2000. Structural Analysis Program, Computers and Structures Inc., Berkeley, California. 2020.
[44] AASHTO 2005. AASHTO LRFD Bridge Design Specifications. American Association of State Highway and Transportation Officials, Washington DC. 2005.